

Fickian and Case II diffusion of water into amylose: a stray field NMR study

I. Hopkinson^{a*}, R. A. L. Jones^a, S. Black^b, D. M. Lane^b and P. J. McDonald^b

^aPolymers and Colloids Group, Cavendish Laboratory, University of Cambridge, Cambridge CB3 0HE, UK

^bDepartment of Physics, University of Surrey, Guildford, Surrey GU2 5XH, UK

(Received 22 January 1997; revised version received 20 May 1997; accepted 28 May 1997)

The ingress of liquid water and water vapour into glassy pellets of the starch polymer amylose has been studied using stray field nuclear magnetic resonance imaging (STRAFI), to produce one-dimensional water concentration profiles as a function of depth from the sorption surface, and time. For the vapour experiments the observed concentration profiles are characteristic of a system showing Fickian diffusion with a mutual diffusion coefficient, a function of the concentration of the penetrant. In contrast, the ingress of liquid water is non-Fickian; concentration profiles characteristic of Case II diffusion have been modelled semi-quantitatively using the Thomas–Windle model. © 1997 Published by Elsevier Science Ltd. All rights reserved

INTRODUCTION

The ingress of water into starch is of interest because it has relevance to the storage, drying and processing of starch-containing materials, which are important in the food industry. The presence of unintended amounts of water can lead to loss of eating quality and microbial spoilage. The distribution of water in a system also has an influence on the cooking and flavour release properties.

In this work we study the behaviour of amylose, which is a linear, amorphous polysaccharide found in starch, with a molecular weight in the range 10^5 – 10^6 . The hope is that results from the amylose–water system may be more generally applicable to other hydrophilic polymer systems, and be of use in understanding multicomponent food systems. The importance of the glass transition in food materials has been recognised and the whole approach to starch-containing systems as being essentially analogous to synthetic polymer systems is gaining currency (Blanshard and Lillford, 1993). It is known that the glass transition temperature, T_g , of starch varies as a function of water content and that the variation of T_g with water content can be predicted using the Couchmann–Karasz equation (Kalicevsky *et al.*, 1992). The plasticization of starch by water is not unique, very similar behaviour

is seen for other food polymers such as gluten (Noel *et al.*, 1995), maltose (Parker and Ring, 1995) and casein (Kalicevsky *et al.*, 1993). For amylose we would expect the glass transition to fall at room temperature for some composition in the range 0.1–0.3 dry weight water content (Slade and Levine in Blanshard and Lillford (1993), Kalichevsky *et al.* (1992)). The significance of this observation is that for the range of water contents encountered in these experiments we would expect the amylose to go from a glassy solid at low water content to a rubbery solid after sorption at unit water activity. This change from glassy to rubbery solid will have a profound effect on both the mutual diffusion coefficient and the viscoelastic response of the amylose–water system which, in turn, affect the transport properties of the system.

For many systems, classical Fickian diffusion, which is characterised by kinetics which are linear in square root of time, is observed. However, in the case of many penetrant polymer systems Fickian kinetics are not observed because the transport process is limited by the swelling of the polymer matrix to accommodate the penetrant, i.e., the viscoelastic properties of the matrix become important, in this situation so-called case II diffusion may be observed. The defining characteristic of case II diffusion is that the mass uptake is linear with time rather than linear with square root time. In addition the shape of the penetrant ingress profile is often very distinctive; it is virtually a step function with

*To whom correspondence should be addressed.

the region preceding the 'front' having a low penetrant concentration and the region behind the front having a constant, equilibrium composition. We note that in fact a continuum of behaviours is seen with time exponents between 0.5 (Fickian) and 1.0 (case II). The situation here, with the transition between glassy and rubbery solid lying within the expected composition range, is one in which case II transport would be expected.

A theoretical description of case II diffusion has been provided by Thomas and Windle (1982); this approach has been used to model diffusion in the poly (methyl methacrylate)/methanol (Thomas and Windle, 1982) and polystyrene/iodohexane (Hui *et al.*, 1987a, b) systems using the Thomas–Windle model. Thus, an important question to ask is under what circumstances the ingress of water into amylose follows case II kinetics, rather than generalised Fickian kinetics, albeit with the diffusion coefficient being a strong function of water concentration. These questions can be addressed in part using gravimetric experiments (Fish, 1957); however, the interpretation of such data can be ambiguous and a more powerful approach is to study the development of the water vs depth profile as a function of time. These data can be analysed using the Boltzmann transform (Crank, 1975), and numerical solution of the diffusion equation, or using the Thomas–Windle model in the event of case II diffusion.

Conventional nuclear magnetic resonance imaging (MRI) (Callaghan, 1991) using switched field gradients has been used to study the ingress of water into pasta (Hills *et al.*, 1996) and nylon (Mansfield *et al.*, 1992), as well as whole wheat grains (Stapley, 1995). The drawback of this method is that it is difficult to image systems with short spin–spin relaxation times (T_2), including solid materials and penetrants at low concentrations. This difficulty arises because maintaining resolution in short T_2 systems requires that high field gradients must be applied for short times and switched correspondingly fast, the conventional MRI of short T_2 systems, therefore, poses serious technical challenges. For this work we use stray field NMR imaging (STRAFI), which has been developed in the last few years following the original work of Samoilenko *et al.* (1988). This technique has been specifically developed for high spatial resolution imaging of short T_2 systems. A more detailed account of the STRAFI experiment can be found in Benson and McDonald (1995). The basis of STRAFI is to place the sample of interest in a high, linear field gradient, such as is found surrounding a high field magnet. A broad-band radio frequency pulse is used to excite a thin slice of the sample, typically 7–70 μm , depending on the pulse length and the gradient strength. To obtain a profile of the sample it is moved within the field gradient to excite successive slices and so build up a one-dimensional profile in the gradient direction. Profiles generally took of the order of 10 min

to collect, primarily because the sample was held stationary for each measurement. Profiles can be acquired more rapidly with continuous sample movement, although this complicates the data interpretation (Benson and McDonald, 1995). The drawback of the STRAFI method is that it requires a high band width experiment and thus sacrifices signal to noise considerably when compared with conventional liquid state long T_2 experiments.

EXPERIMENTAL

Disks of corn starch amylose with diameter 6.5 mm and thickness 1 mm were prepared by compression moulding. The corn starch amylose was obtained from Aldrich (catalogue number A7043) and was Soxhlet extracted using methanol to remove free lipid. Two-gram batches of the powdered polymer were mixed with 0.2 g of water and liquid nitrogen using a pestle and mortar. The resulting powder was then placed in a mould and heated to a temperature of 100°C at a pressure of 10–15 MPa and held for 10 min and then cooled, still under pressure, before being removed from the mould at a temperature of approx. 35°C. This is based on the method of Kalichevsky *et al.* (1992). The samples obtained were clear and transparent, we take this to mean that a continuous glassy polymer matrix has been formed; if the sample was simply a compressed powder it would be opaque due to scattering from particle surfaces.

Preliminary gravimetric experiments showed that samples were equilibrated at unit water activity in approx. 5–6 days. Samples were equilibrated at various other water activities by storing them over saturated solutions (Winston and Bates, 1960) and silica gel. Figure 1 shows the sorption isotherm for the amylose used, along with a fit using the (empirical) Oswin equation (Bassal *et al.*, 1993):

$$\phi = A \left(\frac{a_w}{1 - a_w} \right) B, \quad (1)$$

where a_w is the water vapour activity, A and B are empirical factors (determined to be $A=0.21$ and $B=0.14$) and ϕ is the equilibrium water content in the amylose (expressed in g/g dry weight). The dry masses of the sample were obtained by heating the samples to 95°C in a vacuum oven for 24 h. The Oswin equation was used principally because of its simplicity (for subsequent modelling the inverse function, $a_w(\phi)$, is also required) and its ability to describe a wide range of sorption isotherms and although it exhibits an asymptote at $a_w=1$ it describes the data at low activity well.

To measure the ingress of water vapour, samples that had been stored over a silica gel desiccator at 20°C for 2 weeks were glued by one large face to poly (tetrafluoroethylene) (PTFE) plugs which were then

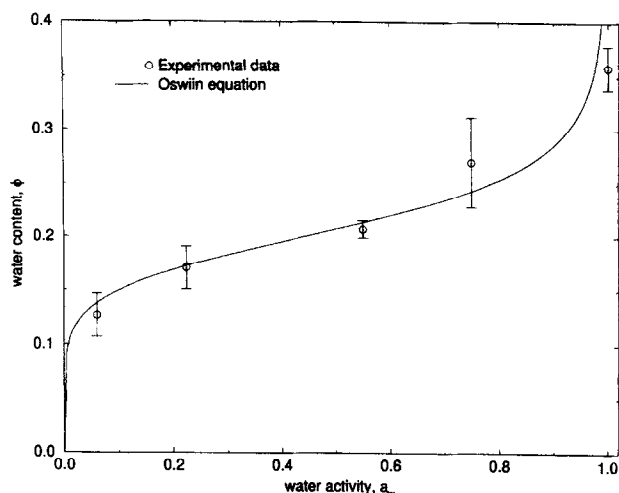


Fig. 1. Sorption isotherm for amylose, with fit using the Oswin equation. Parameters, $A=0.21$, $B=0.14$.

inserted into 7 mm internal diameter glass wells. The wells were filled with distilled water to 3 or 24 mm from the sample surface. This distance will be referred to as the sample/water gap. To constrain the water vapour to enter the sample solely through the front face, silicone grease was applied to the edges of the sample. The silicone grease does contribute to the observed signal, however, it does not penetrate into the sample. A profile was measured for each sample before the addition of the water in order to establish the relative contributions made by the grease, background amylose and residual water. All measurements were made at 20°C. The sample mass was recorded before and after each sorption experiment. During ingress the samples swelled in both the radial direction and in the direction of ingress, although the degree of swelling was relatively small.

One-dimensional profiles were obtained all the way through the sample. At each 50 μm slice the sample was held stationary and 16 quadrature echoes were recorded, using the $90_x-\tau-(90_y-\tau-\text{echo}-\tau)_n$ pulse sequence with $\tau=50\ \mu\text{s}$, where 90_x is a 90° radio frequency excitation pulse of relative phase x . Each profile of $80\times 50\ \mu\text{m}$ consisting of 64 averages took 20 min to acquire and up to 48 profiles were acquired for each sample. The 16 quadrature echoes form a multi-exponential decay train, there being a component for each of the amylose, water and grease. Their intensities reflect hydrogen density and the decay times hydrogen mobilities.

Experiments to study the ingress of liquid water were performed by embedding the amylose pellets in the base of the wells used for the vapour experiments, leaving the top face uncovered. Distilled water was then injected onto the top of the amylose pellet and one-dimensional profiles were obtained in a manner similar to that used for the vapour ingress experiments, but with a 100 μm slice size which resulted in an acquisition time of

approx. 10 min per profile. It was not possible to measure the water content of the pellets after liquid ingress because of extensive disruption of the sample caused by the ingress.

RESULTS

We will start by considering the vapour ingress experiments. Our aim is to obtain water content profiles from the raw STRAFI data. The echo trains collected reflect the spin-spin relaxation behaviour of the sample, which will contain contributions from a number of components which may all change with water content. However, since only a limited number of quadrature echoes were collected and the signal to noise ratio is relatively poor, it is not possible to make a detailed determination of all of these components and so we will attempt to determine an empirical relationship between NMR signal and water content.

Firstly, contributions from the grease component must be accounted for, the preferred way of doing this is to fit the initial sample/grease echo trains to a multicomponent exponential to identify the grease component. This can then be subtracted from all subsequent data sets prior to further analysis. The advantage of this method is that it is insensitive to changes in the relaxation time of the sample as, for instance, the water content varies. This procedure is, however, sensitive to noise in the initial profile, in practice, because the grease signal dominates the initial profile of the nearly dry sample, it is statistically more appropriate to subtract the data from the initial sample from subsequent data for which sorption was occurring. On inspection it was found that the echo intensities after the subtraction of the background, $M(n)$, of each slice could be described by the expression:

$$M(n) = M(0)\exp\left(\frac{-2n\tau}{T_2^{\text{eff}}}\right), \quad (2)$$

where τ is the pulse gap and n is the echo number. T_2^{eff} is an effective spin-spin relaxation time. Thus, the echo intensities acquired for each slice were fitted to exponential decays in order to yield $M(0)$ for each slice, which gives a better measure of the hydrogen content. We note that if the extrapolation to obtain $M(0)$ is carried out before the background subtraction and the $M(0)$ profiles used in the subtraction procedure, then essentially the same profiles are obtained, however, they exhibit rather larger statistical errors. This is because an echo train with contributions from grease, amylose and water would be better represented by more than one exponential decay. Experiments on equilibrated samples showed that $M(0)$ varied linearly with water content over the range of water contents observed here, this is shown in Fig. 2. $M(0)$ will deviate from linearity at some point

below 0.1 water content because there must be some residual signal from completely dry amylose. Such linear behaviour has also been reported for whole wheat grains by other workers (Stapley, 1995) and so the $M(0)$ profiles were converted to profiles of water content using a linear relationship. For samples with a 3 mm sample/water gap the total water content of the sample changed from 0.10 to 0.20 during the course of the experiment. The samples swelled by approximately 5% in the ingress direction during the course of the experiment, no correction has been made for this relatively minor amount of swelling.

Figure 3(a) shows selected $\phi(z)$ profiles as a function of time, $z=0$ was set to coincide with the maximum in $\phi(z)$, because of resolution effects the apparent $\phi(z)$ passes through a maximum near but not at the sample surface. The uniform increase in water content beyond the diffusion 'front' indicates that despite the application of silicone grease to the sample edges some ingress of water occurred through the sides of the sample.

Since it was not possible to measure the mass uptake of water during the liquid ingress experiments it was not possible to obtain profiles of water content vs depth. Figure 3(b) shows plots of magnetisation, $M(0)$ (in arbitrary units) vs depth as a function of time. These profiles include contributions from the mounting glue and the liquid water on top of the sample. The surface of the sample is at 0.0 on the depth axis and for depth less than zero the signal is from liquid water. The signal is not constant in this region and rises on reaching the sample because of T_1 effects. The acquisition was optimised to observe the water in the starch region, where T_1 is very short, this means that the signal from the water, where T_1 is much longer, is reduced by saturation effects. It is clear from these plots that the ingress of liquid water into amylose is much more rapid than the ingress of water vapour and that the epoxy glue prevents the side ingress of the liquid water.

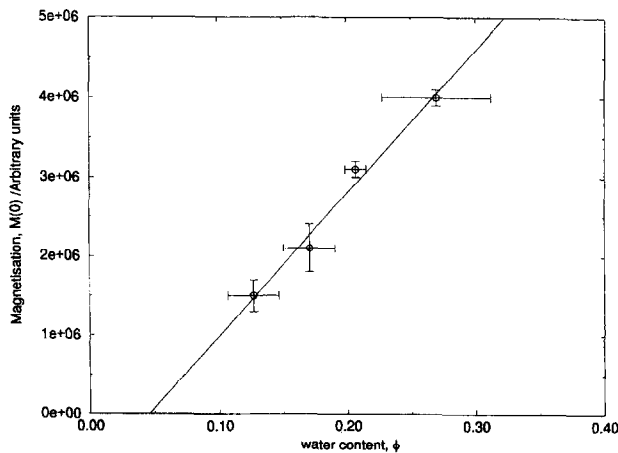


Fig. 2. Measured magnetisation, $M(0)$, in arbitrary units as a function of water content. Line is a linear fit.

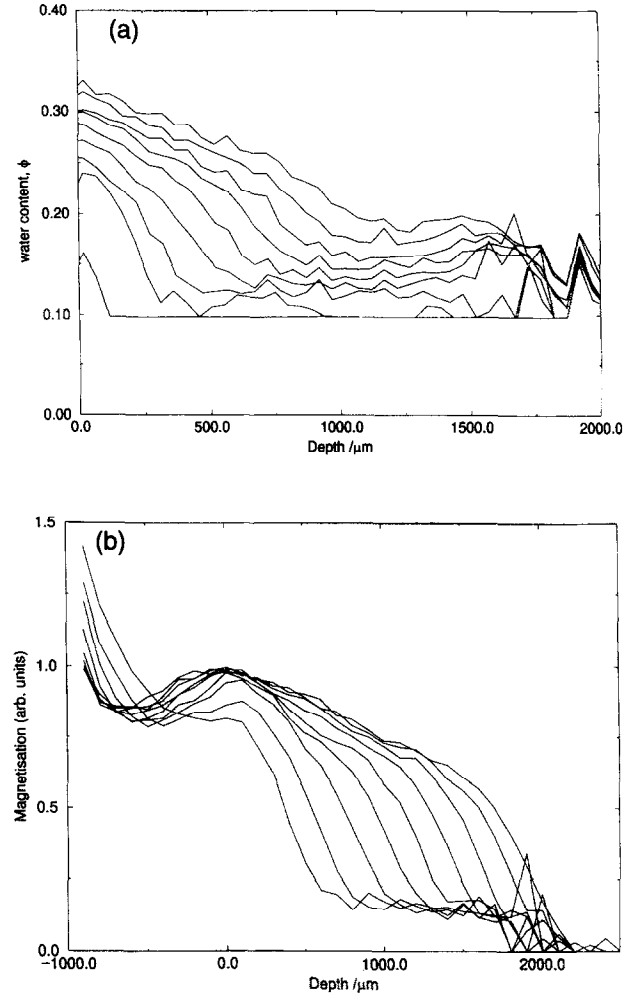


Fig. 3. (a) Water content profiles, $\phi(z)$, as a function of time, for vapour ingress experiments with a 3 mm sample/water gap data. Time between successive profiles is 100 min, starting at zero time, ingress is from left. (b) Magnetisation profiles, $M(z)$, as a function of time, for liquid ingress experiments. Time between successive profiles is 10 min, ingress is from left.

DISCUSSION

One of the main questions of interest in this work was whether the ingress of water into amylose was case II and could be described by the Thomas–Windle model, or whether it could be described by the general form of the Fickian equation:

$$\frac{\partial \phi(z)}{\partial t} = \frac{\partial}{\partial z} D(\phi) \frac{\partial \phi(z)}{\partial z}, \quad (3)$$

where $\phi(z)$ is the water mass fraction profile and $D(\phi)$ is the mutual diffusion coefficient, which is a function of the water mass fraction.

The vapour ingress and liquid ingress experiments exhibit quite different behaviour. A powerful test of the nature of the diffusion is to measure the front position as a function of time. Case II transport is characterised by a front that propagates linearly with time and

Fickian diffusion is characterised by a front that propagates linearly with the square root of time. Figure 4(a, b) show the front position at half height, λ , for the vapour and liquid experiments, respectively, along with fits of the form:

$$\lambda = At^n \quad (4)$$

where A and n are fitting parameters, also included in these figures are model predictions for the front positions derived from models described below. For the vapour ingress, a value of $n=0.53(1)$ is fitted and for the liquid ingress $n=1.09(3)$ is obtained. This indicates that transport is Fickian for the vapour ingress and case II for the liquid. Note that in saying this we do not imply that the state of the water in the amylose is different, simply that in one case water molecules are supplied from vapour and in the other from liquid.

Looking first at the vapour experiments in more detail the surface water content, $\phi(0)$, as a function of time is shown in Fig. 5. Such behaviour is observed if the transport of water vapour to the surface of the sample is a limiting factor (Halse, 1996). To confirm that this was the case, an experiment was run with a sample/water distance of 24 mm. The water uptake in this experiment was much slower than that for the 3 mm sample/water gap. This is reflected in the surface water content, $\phi(0)$, which is the lower trace shown in Fig. 5. This indicates that the diffusion process is limited by the transport of the water vapour to the amylose surface. Although the diffusion coefficient of water in the vapour phase is much more rapid than in the amylose, the equilibrium water content in the amylose is around 4 orders of magnitude higher than in the vapour, and so the relative flux to the sample surface is small.

Given that the diffusion from the vapour is Fickian, it is possible to obtain $D(\phi)$ analytically using the change of variable $z \Rightarrow z t^{-1/2}$, known as the Boltzmann transform (Crank, 1975), in which case:

$$D(\phi) = -\frac{1}{2} \left[\frac{\partial \xi}{\partial \phi'} \right]_{\phi_0}^{\phi} \int_0^{\phi} \xi d\phi', \quad (5)$$

where $\xi = z t^{-1/2}$. In the common case where $\phi(0)$ is constant with time, it is possible to superimpose diffusion profiles collected at different times by the use of this transform. For $\phi(0)$ as a function of time Eq. (5) is not exact because the boundary condition at this surface cannot be expressed solely in terms of ξ . However, if $(d\phi(0)/dt)$ is relatively small the errors introduced by using it are not large. We check that this is so by directly solving Fick's equation for the derived $D(\phi)$ and comparing with the original profiles. Figure 6(a) shows $D(\phi)$ that have been calculated by applying the Boltzmann transform to quadratic fits of the concentration profiles collected at various times. These quadratic fits were limited so as not to include the part

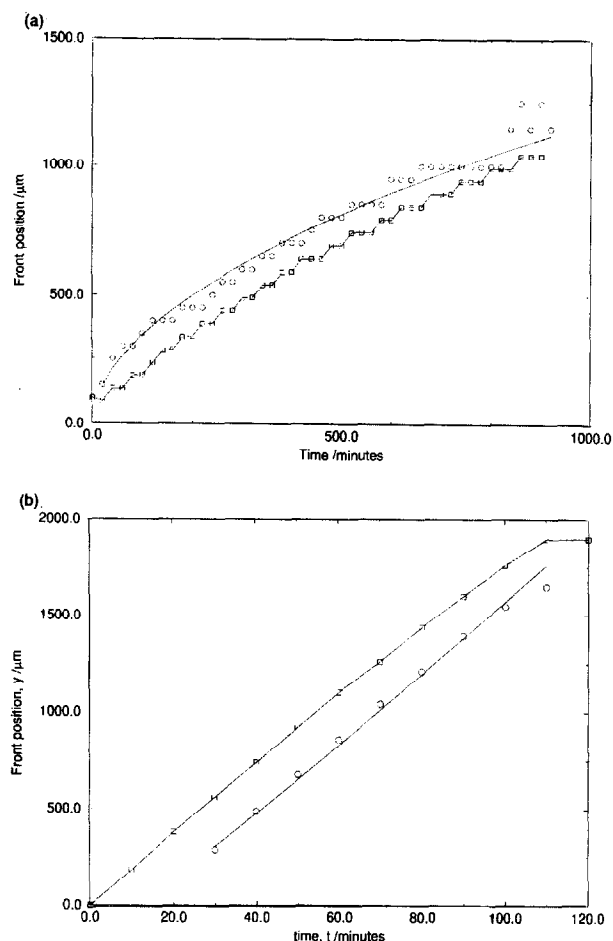


Fig. 4. (a) Measured front position as a function of time (circles), with a power law fit (line), and model result (squares) for the vapour ingress experiment with a 3 mm sample/water gap data. Model results are from the Fickian model described in the Discussion section. (b) Measured front position as a function of time (circles), with a power law fit (line), and model result (squares) for the liquid ingress experiment. Model results are from the Thomas–Windle model described in the Discussion section.

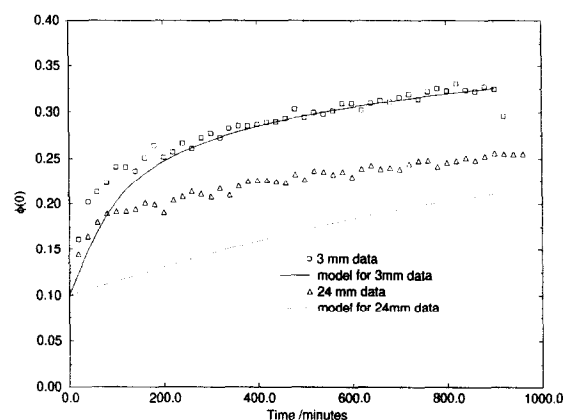


Fig. 5. $\phi(0)$ vs time for 3 mm sample/water gap samples and 24 mm sample/water gap sample, with model predictions using $D_w = 2.5 \times 10^{-5} \text{ m}^2 \text{ s}^{-1}$.

of the profile that is dominated by the side ingress, i.e., for later times, $\phi < 0.18$. However, the Boltzmann transform requires an integration from zero concentration and so values for these lower concentrations are obtained by extrapolation of the quadratic fits. The calculated $D(\phi)$ appear to vary quite considerably depending on the diffusion time, profiles collected at longer times often give negative values of $D(\phi)$ for $\phi < 0.1$, this occurs when the extrapolation of the quadratic fit exhibits a maximum for $\phi < 0.1$. Figure 6(b) shows an 'average' $D(\phi)$, this was calculated by averaging $D(\phi)$, excluding those profiles obtained at later times from the average at lower ϕ and excluding those profiles collected at shorter times from the average at larger ϕ . This was done in order to try and reduce the effect of extrapolation on the average, and is in some respects a subjective process. This average $D(\phi)$ is compared with the data from Fish (1957) acquired using gravimetric methods, along with a theoretical prediction described below.

In order to check the influence of the $D(\phi)$ on observed profiles and check the validity of the assumption that variation in $\phi(0)$ with time is caused by a vapour phase transport, Eq. (3) was solved numerically using standard methods. The boundary condition at $z=0$ was modelled using Fick's Law:

$$F = -D_w \left(\frac{w_1 - w_0}{g} \right), \quad (6)$$

where F is the flux of water into the front face of the sample, D_w is the self diffusion coefficient of water in the vapour, w_0 and w_1 are the concentrations of water in the vapour phase immediately above the water surface and immediately adjacent to the amylose surface, respectively, and g is the sample/water gap. w_1 is obtained by assuming that the vapour immediately adjacent to the amylose surface is in equilibrium with the surface layer of the sample. This equilibrium is described by the sorption isotherm shown in Fig. 1, fitted using the Oswin equation. The mass concentration of water in the vapour near the amylose surface, w_1 , is simply the product of the activity, a_w , and the saturated mass concentration, w_0 . Figure 5 shows the comparison between $\phi(0)$ for the experimental data and from numerical solutions using the literature value (Lide, 1995) for $D_w (= 2.5 \times 10^{-5} \text{ m}^2 \text{ s}^{-1})$. This works well for the 3 mm sample/water gap data, however, there is a large discrepancy for the 24 mm sample/water gap data. This suggests that there is an additional water transport mechanism, other than self diffusion, such as convection taking place in the larger sample/water gap.

Concentration profiles calculated using the average $D(\phi)$ discussed earlier and the $D(\phi)$ measured by Fish (1957) are compared, in Fig. 7, to experimentally determined concentration profiles measured at 200 and

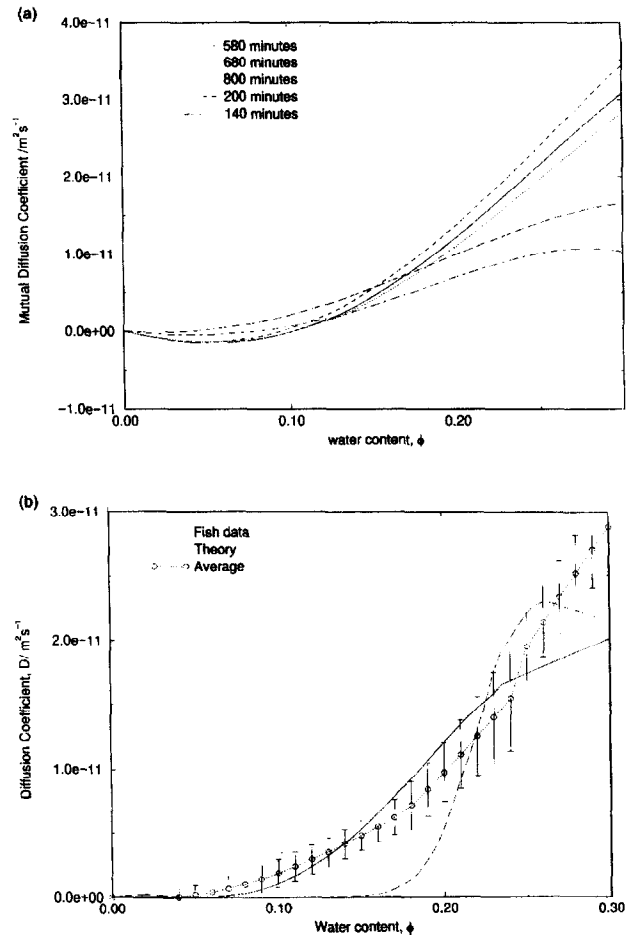


Fig. 6. (a) Mutual diffusion coefficient, $D(\phi)$, for water in amylose as a function of water content; individual curves are calculated from data collected at the times shown. (b) Mutual diffusion coefficient for water in amylose as a function of water content from this work (average value), gravimetric experiments by Fish (1957) and from theoretical calculations using the self diffusion coefficient.

800 min diffusion time. Concentration profiles calculated from the individual mutual diffusion coefficient shown in Fig. 6(a) are broadly similar to those calculated using the average $D(\phi)$. Included in Fig. 4(a) is the front position calculated from this model using the average $D(\phi)$, the trend of the experimental data is matched well although there is an offset between the experimental and model calculations. This offset arises from two effects; firstly, the side ingress will shift the position of the front, and secondly the sample surface is not precisely defined. Clearly, if one were able to observe the ingress with a sample which was initially dry and side ingress were reduced, then the $D(\phi)$ calculated would be more accurate. The method used here to obtain the mutual diffusion coefficient function has several advantages over the gravimetric method. Firstly, the data analysis is relatively model free; secondly, it provides more information on the diffusion process than gravimetric data; and finally, the measurement is quick and

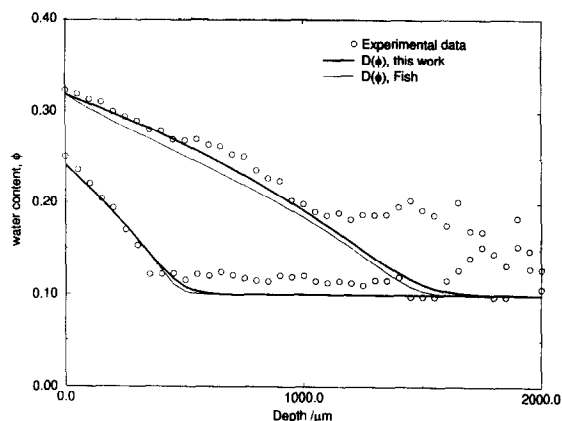


Fig. 7. Ingress profiles (symbols) for 200 and 800 min with simulated profiles using $D(\phi)$ from Fish (1957), and the averaged $D(\phi)$ from this work.

easy—in principle, the mutual diffusion coefficient could be measured from a single profile.

Theories exist (Duda *et al.*, 1979; Kuhn and Lechert, 1990) that describe the relationship between the self diffusion coefficient and the mutual diffusion coefficient, the link being the sorption isotherm. Figure 6(b) includes the predicted $D(\phi)$ for this system, using the theory of Duda *et al.* (1979), the sorption isotherm and the self diffusion coefficients obtained by Kuhn and Lechert (1990) using NMR measurements. The agreement with data from the current work and the work of Fish (1957) is fair. The weak link in the calculation is the self diffusion measurements, which are calculated indirectly from the relaxation times T_1 and T_2 . The more direct NMR method for obtaining self diffusion coefficients (Callaghan, 1991) is difficult to apply to this system because of the low water content.

In the past, the Thomas–Windle model has been successfully used to describe the ingress of penetrants into synthetic polymers. Here we will try to apply the model to the amylose–water system. We will describe how we estimated initial parameters for the model and present model results for values of these parameters that have been adjusted manually to give a somewhat better fit to the experimental data. For the liquid ingress experiments, the absolute water content of the sample is not known. This presents something of a problem; here we chose to normalise both experimental and model profiles such that the initial water content is 0.1 and the final water content is 1.0. This scaled water content probably corresponds quite closely to the dry weight content since we know that the initial water content is around 0.1 and separate gravimetric experiments on extruded starch material suggest a water content of between 0.8 and 1.0 for samples left in water for a comparable time. A very brief outline of the model will be presented here in order to define the necessary input parameters. Details of the model can be found in Thomas and Windle (1982). The basis of

the Thomas–Windle model is to divide the transport process into two steps:

- (1) The diffusion of penetrant into the matrix (this is a Fickian process).
- (2) The swelling of the matrix to accommodate the penetrant molecule.

The coupled pair of equations that these two processes produce are solved using finite difference methods. The activity profile, a , and the volume fraction of penetrant normalised by the equilibrium volume fraction, v , are calculated. The swelling of an element is described by:

$$\left(\frac{dv}{dt}\right)_i = -\frac{RT}{V_1 N_A k \eta_0} \ln\left(\frac{v}{a}\right)_i e^{Mv} \quad (7)$$

for the rate of swelling of an element i from the surface, where: $V_1 N_A$ is the molar volume of water, R is the gas constant, T is the absolute temperature, k is the ratio ε/v , where ε is the strain.

The kinetics of swelling of the matrix are assumed to be described by a single dilational viscosity, represented by the function:

$$\eta = \eta_0 e^{-Mv} \quad (8)$$

where η_0 and M are empirical parameters. η_0 will determine the magnitude of the viscosity and M determines how rapidly the viscosity decreases with increased water content, clearly the viscosity will vary strongly with the water content. The diffusion step is described by Fick's Law, with D the composition-dependent mutual diffusion coefficient.

k Can be obtained by measuring the swelling of a sample for a known normalised water content, v ; we have measured this value for extruded amylose/amylopectin mixtures and obtained a value of 0.23 and this is consistent with the swelling observed for the pure amylose samples used in the ingress experiments. Interestingly, this is comparable with the value quoted by Thomas and Windle (1982) for the poly (methyl methacrylate) (PMMA)/methanol system.

We can obtain a crude estimate for the order of magnitude for η from the work of Villar *et al.* (1995), who measured the viscosity of starches with various amylose contents, along with the temperature dependence over the range 140–170°C and water + glycerine contents of around 0.23. Extrapolating these data back to 20°C, a value of $\eta_0 = 1.5 \times 10^{13}$ Pa s is obtained assuming that $M = 15$, as is the case in the PMMA/methanol system and that glycerine has the same plasticising effect as the equivalent amount of water. It is this estimation of η_0 that is the most uncertain element in the calculation; owing to both the long extrapolation in temperature and the assumption regarding the plasticising effect of glycerine.

We have obtained a quadratic fit to $D(\phi)$ for the starch–water system in the vapour ingress experiment

over the water content range 0.1–0.3. For water contents greater than 0.3 we have two options:

- (1) Extrapolate from the values of the diffusion coefficient obtained in the lower water content range. This is somewhat undesirable since we have no indication as to the form the extrapolation should take and from a practical standpoint we have no simple way of varying the value of D in this region.
- (2) Use a fixed value of the mutual diffusion coefficient, D_2 , for the water content range 0.3–1.0. Fish (1957) shows the value of the mutual diffusion coefficient plateauing at a value of $2.5 \times 10^{-11} \text{ m}^2 \text{ s}^{-1}$ for potato starch gels, although a maximum water content of only 0.4 is considered. Ohtsuka *et al.* (1994) have used NMR methods to measure self diffusion coefficients for potato starch gels with water contents of 2.4–5.9 (dry mass content), obtaining values of $4.7 \times 10^{-10} \text{ m}^2 \text{ s}^{-1}$ – $1.4 \times 10^{-9} \text{ m}^2 \text{ s}^{-1}$ in this range. The advantage of this method is that D_2 can be adjusted in a straightforward manner.

We will choose to take this second option with an initial value of $D_2 = 1 \times 10^{-10} \text{ m}^2 \text{ s}^{-1}$, on the grounds that this makes the minimum number of assumptions about the behaviour of the diffusion coefficient in the higher water content region and the initial value is intermediate between the values obtained for high water content starch gels and lower water content potato tissue.

Using the Thomas–Windle model with these initial parameters gives a fair qualitative fit to the experimental data. It indicates that case II behaviour should be expected and the predicted front velocity is within an order of magnitude of the observed velocity. Changing the value of M , whilst remaining consistent with the viscosity data from Villar *et al.* (1995) results in relatively minor changes in the front velocity and shape. It is also found that using extrapolating values of the diffusion coefficient for water contents above 0.3 gives quite similar results to those obtained using a fixed value for the diffusion coefficient above 0.3, as long as the value of D_2 is fixed at the value of the extrapolated function for water content 1.0.

Adjusting the values of η_0 and D_2 manually gives values of $0.65 \times 10^{13} \text{ Pa s}$ and $5.0 \times 10^{-10} \text{ m}^2 \text{ s}^{-1}$. These values reproduce the front velocity well, as can be seen in Fig. 4(b). Again the absolute front position is systematically offset, probably due to difficulties in defining exactly the sample surface. Figure 8 shows a comparison between experimental profiles and model profiles for the same ingress time. The model reproduces the slope in the region behind the front, this slope behind the front is determined mainly by the value of D_2 . The front shape is not reproduced well, the experimentally determined front being rather

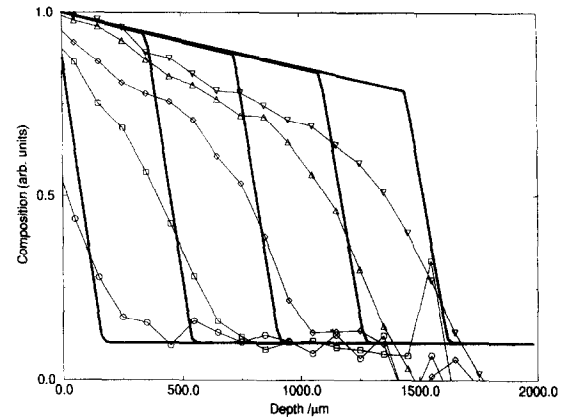


Fig. 8. Comparison of experimentally determined ingress profiles for liquid ingress with profiles calculated using the Thomas–Windle model. The vertical scale is in arbitrary units. Profiles are shown at 20 min intervals. Filled symbols are model data, open symbols experimental data for the same ingress time.

shallower in slope than the model front—this is despite the fact that the model accounts for the smearing of the front which arises because the front moves significantly during the profile acquisition time. One possible explanation for this difference in front shape is that in terms of the NMR measurement the sample does not relax immediately to its equilibrium condition, so the front shape is distorted by sample relaxation effects. In addition, the Thomas–Windle model contains a number of approximations that may influence the predicted profile shape. The induction time predicted by this model is of the order of 10 min; this means that the induction period cannot be probed in detail using STRAFI. In principle, it should be possible to model both the vapour ingress and liquid ingress consistently using a single Thomas–Windle style model and applying a flux limitation in the case of the vapour ingress. In practice, we have been unable to do this; profiles produced are more Fickian in appearance, i.e., they do not exhibit a sharp front, however, the kinetics are still characterised by a time exponent of 1.0, characteristic of case II diffusion. This may be because of shortcomings in the Thomas–Windle model, or it may be that the balance between Fickian and case II kinetics is quite fine and that the parameters sufficient to model the case II behaviour for the liquid ingress are not quite those required to model both Fickian and case II behaviour consistently.

CONCLUSIONS

The ingress of water into amylose as a function of time has been followed using stray field NMR. The profiles obtained using vapour as the water source have been fitted using a general Fickian model of the diffusion process with a boundary condition accounting for the

transport of water in the vapour phase. The mutual diffusion coefficient, $D(\phi)$, shows a continuous monotonic increase in the composition range covered (0.1–0.3 dry weight). The behaviour observed for the ingress of liquid water is characteristic of case II transport and has been modelled using the Thomas–Windle model. This model predicts the right type of behaviour using reasonable input data from the literature and from the vapour ingress experiments. Optimising these parameters improves the match between theory and experiment, although the profile shape is not predicted exactly. This could be due to NMR relaxation effects influencing the detailed shape of the profiles or due to approximations in the Thomas–Windle model. These experiments have illustrated the use of a new technique to study the problem of water transport in amylose; this technique should be applicable to a wide range of low water content systems.

ACKNOWLEDGEMENTS

Support for IH and RALJ was provided by the BBSRC; we all thank the EPSRC for funding the stray field NMR facility at the University of Surrey (Grant Number GR/K12397).

REFERENCES

- Bassal, A., Vasseur, J. and Lebert, A. (1993) Measurement of water activity above 100°C. *Journal of Food Science* **58**, 449–452.
- Benson, T. B. and McDonald, P. J. (1995) Profile amplitude modulation in stray-field magnetic-resonance imaging. *Journal of Magnetic Resonance A* **112**, 17–23.
- Blanshard, J. M. V. and Lillford, P. J. (1993) *The Glassy State in Foods*. Nottingham University Press, Nottingham.
- Callaghan, P. T. (1991) *Principles of Nuclear Magnetic Resonance Microscopy*. Oxford University Press, Oxford.
- Crank, J. (1975) *The Mathematics of Diffusion*. Oxford University Press, Oxford.
- Duda, J. L., Ni, Y. C. and Vrentas, J. S. (1979) An equation relating self-diffusion and mutual diffusion coefficients in polymer-solvent systems. *Macromolecules* **12**, 459–462.
- Fish, B. P. (1957) *Diffusion and Equilibrium Properties of Water in Starch*. Her Majesty's Stationery Office, London.
- Halse, M. R. (1996) Personal communication.
- Hills, B. P., Babonneau, F., Quantin, V. M., Gaudet, F. and Belton, P. S. (1996) Radial NMR Microimaging studies of the rehydration of extruded pasta. *Journal of Food Engineering* **27**, 71–97.
- Hui, C.-Y., Wu, K.-C., Lasky, R. C. and Kramer, E. J. (1987a) Case-II diffusion in polymers. I. Transient swelling. *Journal of Applied Physics* **61**, 5129–5136.
- Hui, C.-Y., Wu, K.-C., Lasky, R. C. and Kramer, E. J. (1987b) Case-II diffusion in polymers. II. Steady-state front motion. *Journal of Applied Physics* **61**, 5137–5149.
- Kalichevsky, M. T., Blanshard, J. M. V. and Tokarczuk, P. F. (1993) Effect of water content and sugars on the glass transition of casein and sodium caseinate. *International Journal of Food Science and Technology* **28**, 139–151.
- Kalichevsky, M. T., Jaroszkiewicz, E. M., Ablett, S., Blanshard, J. M. V. and Lillford, P. J. (1992) The glass transition of amylopectin measured by DSC, DMTA and NMR. *Carbohydrate Polymers* **18**, 77–88.
- Kuhn, K. and Lechert, H. (1990) Determination of Fickian diffusion coefficients of water in foods using nmr-techniques and the DARKEN-equation. *Lebensmittel Wissenschaft und Technologie* **23**, 331–335.
- Lide, D. R. (Ed.) (1995) *CRC Handbook of Chemistry and Physics*. CRC Press, London.
- Mansfield, P., Bowtell, R. and Blackband, S. (1992) Ingress of water into solid nylon 6.6. *Journal of Magnetic Resonance* **99**, 507–524.
- Noel, T. R., Parker, R., Ring, S. G. and Tatham, A. S. (1995) The glass-transition of wheat gluten proteins. *International Journal of Biological Macromolecules* **17**, 81.
- Ohtsuka, A., Watanabe, T. and Suzuki, T. (1994) Gel Structure and water diffusion phenomena in starch gels studied by pulsed field gradient stimulated echo NMR. *Carbohydrate Polymers* **25**, 95–100.
- Parker, R. and Ring, S. G. (1995) Diffusion in maltose-water mixtures at room temperatures close to the glass transition. *Carbohydrate Research* **273**, 147–155.
- Samoilenko, A. A., Artemov, D. Y. and Sibel'dina, L. A. (1988) Formation of sensitive layer in experiments on NMR subsurface imaging of solids. *JETP Letters* **47**, 417–419.
- Stapley, A. (1995) PhD Thesis, Department of Chemical Engineering, Cambridge University.
- Thomas, N. L. and Windle, A. H. (1982) A theory of Case II diffusion. *Polymer* **23**, 529–542.
- Villar, M. A., Thomas, E. L. and Armstrong, R. C. (1995) Rheological properties of thermoplastic starch and starch/poly(ethylene-co-vinyl alcohol) blends. *Polymer* **36**, 1869–1876.
- Winston, P. W. and Bates, D. H. (1960) Saturated solutions for the control of humidity in biological research. *Ecology* **41**, 232–237.